Persistence of Structure Over Fluctuations in Biological Electron-Transfer Reactions

Ilya A. Balabin* and David N. Beratan+
Department of Chemistry, Duke University, Durham, North Carolina 27708, USA
Spiros S. Skourtis‡
Department of Physics, University of Cyprus, 1678 Nicosia, Cyprus
(Received 14 July 2008; published 8 October 2008)

In the soft-wet environment of biomolecular electron transfer, it is possible that structural fluctuations could wash out medium-specific electronic effects on electron tunneling rates. We show that beyond a transition distance (2–3 Å in water and 6–7 Å in proteins), fluctuation contributions to the mean-squared donor-to-acceptor tunneling matrix element are likely to dominate over the average matrix element. Even though fluctuations dominate the tunneling mechanism at larger distances, we find that the protein fold is ''remembered'' by the electronic coupling, and structure remains a key determinant of electron transfer kinetics.

DOI: 10.1103/PhysRevLett.101.158102 PACS numbers: 87.15.R−, 85.65.+h, 87.10.−e

Energy transduction in living organisms relies on the generation of transmembrane electrochemical gradients [1]. Throughout biology, this gradient is established by proton transfer that is driven by multistep electron tunneling between electron localizing groups (cofactors) bound to proteins [2]. The structural diversity and thermal motion of proteins and water induce a broad range of static and dynamical disorder, respectively, in electronic interactions. Static disorder arises from the structural diversity available to electron-transfer proteins, with their hierarchy of organization, and the variety of donor and acceptor cofactor binding modes. In this study, by dynamical disorder we mean thermal fluctuations around an equilibrium structure. Developing a theory to link medium disorder to electron transfer (ET) function is a challenge associated with electron tunneling through soft-wet matter [3–8].

In this Letter, we perform a statistical analysis of structural and dynamical disorder in the electron donor-to-acceptor coupling for unimolecular protein-mediated ET reactions (ruthenated redox proteins [9]) and bimolecular water-mediated ET reactions (cytochrome b_5 self-exchange [10]). These ET systems possess diverse tunneling media and structural fluctuations, and they include a broad range of tunneling distances that show single exponential ET kinetics. Our analysis focuses on the distance dependence of disorder effects.

For long distance ET, the high-temperature limit nonadiabatic rate is $k_{\mathrm{ET}} \propto \langle T_{\mathrm{DA}}^2 \rangle \exp(-\Delta G^{\ddagger}/k_B T)$ [11], where T_{DA} is the bridge-mediated donor-acceptor electronic coupling, $\Delta G^{\ddagger}$ is the activation free energy, and the T_{DA} averaging is done over thermal fluctuations. $\langle T_{\mathrm{DA}}^2 \rangle = \langle T_{\mathrm{DA}} \rangle^2 + \sigma^2$ describes the effects of dynamical disorder on the electronic coupling for a particular ET system. The relative magnitude of σ^2 compared to $\langle T_{\mathrm{DA}} \rangle^2$ determines the significance of the dynamical electronic-coupling disorder. When $\langle T_{\mathrm{DA}} \rangle^2 \gg \sigma^2$, the electronic-coupling fluctuations caused by the molecule's motion do not impact electron tunneling. In the opposite limit of large fluctuations, $\langle T_{\mathrm{DA}} \rangle^2 \ll \sigma^2$, the electronic coupling is enhanced by nonequilibrium conformations. The influence of dynamical disorder on the electronic coupling is quantified by the coherence parameter [12–14]:

$$C = \langle T_{\mathrm{DA}} \rangle^2 / \langle T_{\mathrm{DA}}^2 \rangle = [1 + (\sigma^2 / \langle T_{\mathrm{DA}} \rangle^2)]^{-1}. \quad (1)$$

Values of $C \sim 1$ indicate that tunneling is controlled by the average coupling. $C \ll 1$ indicates that tunneling is dominated by coupling fluctuations (strong dynamical disorder).

By structural electronic-coupling disorder (at a given donor-to-acceptor distance R_{DA}), we mean that $\langle T_{\mathrm{DA}}^2 \rangle$ values differ among chemically distinct ET species with the same R_{DA}. The scatter in $\langle T_{\mathrm{DA}}^2 \rangle$ arises from structural variations between the ET species. For example, the different protein folds with specific secondary structure, donor and acceptor structure, and cofactor binding modes create structural diversity. We use the following quantity to characterize structural disorder at the distance R_{DA}:

$$S[\langle T_{\mathrm{DA}}^2 \rangle] = \sqrt{\mathrm{var}[\langle T_{\mathrm{DA}}^2 \rangle]} / \mathrm{avg}[\langle T_{\mathrm{DA}}^2 \rangle],$$
$$\mathrm{var}[\langle T_{\mathrm{DA}}^2 \rangle] = \frac{1}{N-1} \sum_{\gamma=1}^{N} (\langle T_{\mathrm{DA}}^2 \rangle_{\gamma} - \mathrm{avg}[\langle T_{\mathrm{DA}}^2 \rangle])^2. \quad (2)$$

γ denotes ET species with the donor-acceptor distance R_{DA}, N is the number of ET species at that distance, and avg denotes the average of all $\langle T_{\mathrm{DA}}^2 \rangle_{\gamma}$ for that distance. If $S \ll 1$, the scatter in $\langle T_{\mathrm{DA}}^2 \rangle_{\gamma}$ with respect to avg$[\langle T_{\mathrm{DA}}^2 \rangle]$ is small for the particular donor-acceptor distance, and the effect of structural electronic-coupling disorder on the ET rates is not significant. In this case, an average tunneling-barrier model that reproduces avg$[\langle T_{\mathrm{DA}}^2 \rangle]$ gives, to a good approximation, $\langle T_{\mathrm{DA}}^2 \rangle$ for all ET species at R_{DA}. The opposite limit of large scatter (S of the order of 1 or greater) describes a situation of significant structural disorder. In this regime, $\langle T_{\mathrm{DA}}^2 \rangle$ for any single ET species is not representative of the $\langle T_{\mathrm{DA}}^2 \rangle$ values for the other ET species at the

 © 2008 The American Physical Society

same distance. In this regime, an average tunneling-barrier theory cannot describe the electronic couplings of the different ET systems.

Since the sign of T_{DA} can alternate with some molecular geometry changes, the thermal average $\langle T_{DA} \rangle$ reflects the importance of destructive interference among tunneling pathways [10,12,15]. The dependence of σ on tunneling pathways, and on the average molecular geometry of the ET system, is less straightforward to dissect. σ is expected to increase with donor-acceptor distance since large bridges have enhanced fluctuations (see the auxiliary material [16]). Does this mean that structural heterogeneity is reduced by fluctuations?

We examine the dependence of dynamical electronic-coupling disorder [C, Eq. (1)] and of structural electronic-coupling disorder [S, Eq. (2)] on the donor-acceptor distance R_{DA} for water- and protein-mediated ET reactions. We show that there is a critical distance $R_{DA} = R_c$ (different for water and proteins) beyond which dynamical disorder is likely to dominate the electronic coupling of any ET system ($\sigma^2 > \langle T_{DA} \rangle^2$). Further, this critical distance is approximately equal to two length parameters that characterize the bridge medium: the correlation length of thermal bridge motion and the correlation length of the electron's tunneling propagation. Finally, we demonstrate that the observed overall increase in the dynamical disorder with distance does not reduce structural disorder (the heterogeneity of $\langle T_{DA}^2 \rangle$ values). This is because the sensitivity of the electronic-coupling fluctuations σ to molecular structure is as strong as the sensitivity of the average electronic coupling $\langle T_{DA} \rangle$ to molecular structure.

The 24 ruthenated derivatives of cytochrome c, cytochrome b_{562}, myoglobin, and azurin [9] all have activation free energy $\Delta G^{\ddagger} \sim 0$, and thus the ET rates reflect different tunneling propensities. For water-mediated ET, we explored a system of two cytochrome b_5 molecules participating in a water-mediated self-exchange ET reaction. The cytochrome b_5 molecules were positioned in three different porphyrin ring plane orientations (0°, 45°, or 90°) and, for each orientation, 13 different edge-to-edge distances from van der Waals contact to 9 Å (12 to 21 Å metal to metal) [10].

The electronic-coupling calculations were performed using a tight-binding (extended Hückel) one-electron Hamiltonian with standard parameters [17,18] that have been successfully used for coupling estimates [12,19,20]. T_{DA} was calculated for each molecular dynamics (MD) snapshot using

$$T_{DA} = \sum_{ij}^{\text{bridge}} (E_{tun}S - H)_{Di} \tilde{G}_{ij} (E_{tun}S - H)_{jA}, \qquad (3)$$

where $\mathbf{S}$ and $\mathbf{H}$ are the electronic orbital overlap and Hamiltonian matrices, respectively, $\tilde{\mathbf{G}} = (E_{tun}\mathbf{S}^{\text{bridge}} - \mathbf{H}^{\text{bridge}})^{-1}$ is the bridge Green's function, and E_{tun} is the electron tunneling energy [19–22]. The value of E_{tun} was set ~1 eV from the energies of the protein localized states, and T_{DA} depended weakly on that energy.

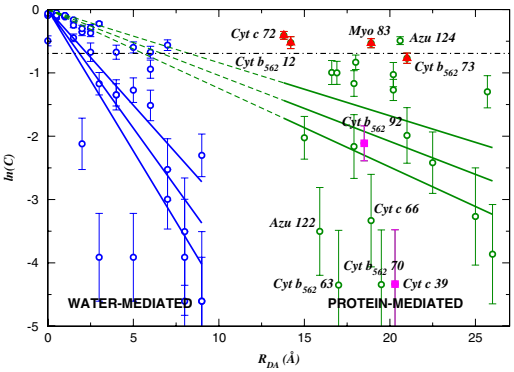

FIG. 1 (color online). Distance dependence of $\ln(C)$ [Eq. (1)] in water- (0 − 9 Å) and protein-mediated (13–26 Å) ET reactions. The solid lines indicate the least squares fits of $\ln(C)$, and its upper and lower estimates. The dashed lines show extensions of the least squares fits for proteins to the anchor at the origin. The dot-dashed line marks $C = 0.5$, for which contributions from $\langle T_{DA} \rangle^2$ and σ^2 are equal.

There were two major sources of sampling errors in the analysis. First, errors arise in the individual $\langle T_{DA}^2 \rangle$ values because of the finite length of the MD trajectories (Figs. 1 and 2). The second source of errors was the finite number of ET species at each distance (Fig. 3). All sampling errors were estimated using bootstrapping with 10 000–100 000 samples [23,24]. Systematic errors associated with the level of electronic structure calculations and classical MD simulations were also present. However, previous work [12,14,19,20] has shown that this computational approach provides reasonable estimates of ET rates in a number of biological systems.

Correlation length of the thermal atomic motion.—To characterize the dynamical disorder of the bridge structure

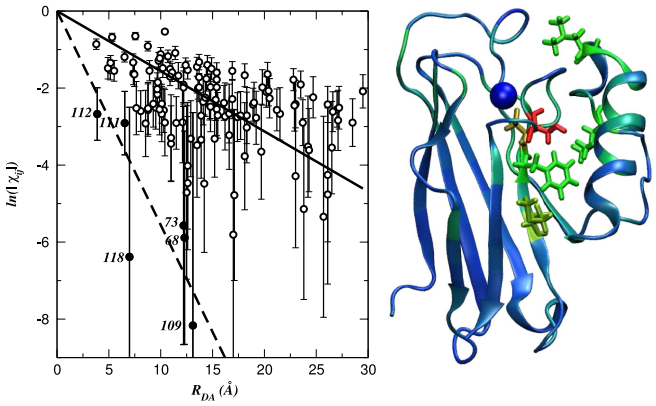

FIG. 2 (color online). Left: Dependence of $\ln(|\chi_{ij}|)$ [Eq. (5)] on the tunneling distance in azurin. The solid line shows the average electronic correlation decay ($R_c = 6.4 \pm 1.5$ Å), and the dashed line is a linear regression for the 6 amino acids with the fastest decay (marked with filled circles and labeled). Right: Protein structure: amino acids with slow and average decays ($R_c = 5$–19 Å) are shown as blue ribbons and tubes, and amino acids with fast decays ($R_c = 1.5$–5 Å) are shown with red, yellow, and green sticks.

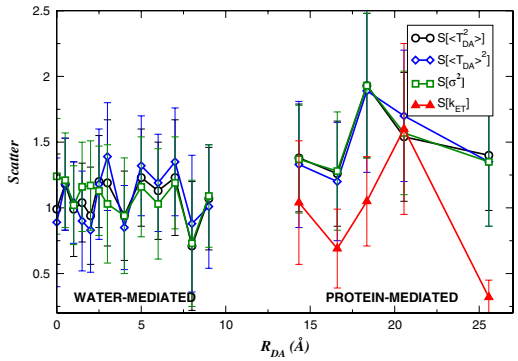

FIG. 3 (color online). Structural disorder parameters $S[\langle T_{DA}^2\rangle]$ [Eq. (2)] (circles), $S[\langle T_{DA}\rangle^2]$ (diamonds), $S[\sigma^2]$ (squares), and $S[k_{ET}]$ (triangles, [9]) as functions of R_{DA}. The error bars describe the errors that arise from the limited number of ET systems at each distance; the errors arising from the finite lengths of the MD trajectories were smaller.

that arises from thermal motion, we computed the atom position covariance matrix κ_{ij} for proteins and water, and studied its dependence on interatomic distance:

$$\kappa_{ij} = \frac{\langle(\vec{r}_i - \langle\vec{r}_i\rangle)(\vec{r}_j - \langle\vec{r}_j\rangle)\rangle}{\sqrt{\langle(\vec{r}_i - \langle\vec{r}_i\rangle)^2\rangle\langle(\vec{r}_j - \langle\vec{r}_j\rangle)^2\rangle}}. \quad (4)$$

$\vec{r}_i$ is the position of atom i, and averaging is performed over each MD trajectory. Calculations of κ_{ij} for proteins included the C_α, C, and N backbone atoms, and the calculations for water included only oxygen atoms. The dependence of κ_{ij} on interatomic distance characterizes the loss of correlation among atomic positions, and reflects the average correlation length for structural fluctuations.

Correlation length of the electron's tunneling propagation.—To explore the loss of memory in the electron's through-bridge tunneling propagation that arises from thermal motion, we calculated the normalized correlation function:

$$\chi_{ij} = \frac{\langle(\tilde{G}_{ii}^2 - \langle\tilde{G}_{ii}^2\rangle)(\tilde{G}_{ij}^2 - \langle\tilde{G}_{ij}^2\rangle)\rangle}{\sqrt{\langle(\tilde{G}_{ii}^2 - \langle\tilde{G}_{ii}^2\rangle)^2\rangle\langle(\tilde{G}_{ij}^2 - \langle\tilde{G}_{ij}^2\rangle)^2\rangle}}. \quad (5)$$

$\tilde{G}_{ij}$ is a matrix element of the bridge electronic Green's function between orbitals i and j and averaging is performed over each MD trajectory. Calculations were performed for wild-type azurin; preliminary results for other proteins are consistent with the azurin observations. The dependence of χ_{ij} on interatomic distance characterizes the loss of correlation among tunneling propagations that involve different distances, and reflects the average correlation length for through-bridge tunneling. To probe dynamic disorder effects throughout the protein, orbital i was taken to be the bridge orbital most strongly coupled to the donor, and orbital j was the σ bond between the C_α and C (carbonyl) backbone atoms of each protein amino acid. A similar metric based on Green's function matrix elements (rather than squares) yielded nearly identical results. In different protein regions, χ_{ij} exhibits different distance dependencies. The difference reflects a connection between structural motifs and the coupling fluctuations related to the motions of the motifs. This connection between structure and electronic-coupling fluctuations is explored further in the following sections.

Dynamic disorder.—Table I shows that a tunneling medium can be characterized by a distance R_c at which a structure-controlled tunneling mechanism ($\langle T_{DA}\rangle^2 > \sigma^2$) is likely to change to a fluctuation-controlled tunneling mechanism ($\langle T_{DA}\rangle^2 < \sigma^2$).

Figure 1 shows the distance dependence of $\ln(C)$, given the fact that dynamical disorder vanishes ($C = 1$, $\ln(C) = 0$) when $R_{DA} = 0$. The distance R_{DA} at which $C = 0.5$ defines a transition distance (R_c) to the fluctuation-controlled regime. R_c was estimated from the data in Fig. 1 using linear regression. The regression analysis was performed for $\ln(C)$ itself and for its upper and lower estimates obtained by bootstrapping [23]. For water-mediated reactions, the correlation coefficient was -0.77, and R_c was estimated to be 1.9 ± 0.4 Å. Proteins showed a relatively small correlation coefficient of -0.26, and R_c was estimated at 6.8 ± 1.2 Å. The structural diversity of proteins leads to a statistical trend characterized by R_c, rather than a clear distance dependence for C.

Figure 2 shows the dependence of $\ln(|\chi_{ij}|)$ on distance in wild-type azurin. The overall distance dependence is nearly exponential, as indicated by the correlation coefficient of -0.78. The correlation length at which χ_{ij} decays to $1/e$ was estimated using the linear regression of $\ln(\chi_{ij})$ anchored at the origin (at zero distance $\chi_{ij} = 1$), and was found to be 6.4 ± 1.5 Å. Some specific protein amino acids deviate from this distance dependence (see auxiliary material [16]). The correlation length estimates using κ_{ij} yielded similar results (see Table I and the auxiliary material [16]).

It is remarkable that the correlation lengths derived from the κ_{ij} and χ_{ij} correlation functions are so close to the transition distances (R_c) derived from $\ln(C)$ (Table I). A related method for deriving R_c by comparing $\langle T_{DA}\rangle^2$ to σ^2 yields similar R_c values (~7 Å for proteins and ~3 Å for water, see the auxiliary material [16]). κ_{ij} and χ_{ij} relate only to the bridge thermal motion while $\langle T_{DA}\rangle^2$, σ^2, and C also contain information about the donor and acceptor

TABLE I. Estimates of the transition distance R_c for proteins and water based on different descriptors. The χ_{ij}-based estimate for water was not computed, because the high mobility of water molecules causes large variations of intermolecular distances over MD trajectories. Estimates based on a comparison of $\langle T_{DA}\rangle^2$ to σ^2 yield $R_c \sim 7$ Å for proteins and $R_c \sim 3$ Å for water.

Descriptor	R_c, proteins (Å)	R_c, water (Å)
$\ln(C)$	6.8 ± 1.2	1.9 ± 0.4
χ_{ij}	6.4 ± 1.5	...
κ_{ij}	6.2 ± 1.4	1.9 ± 0.5

cofactor fluctuations. These results show that, on average, fluctuation-controlled tunneling dominates biological ET for donor-acceptor distances larger than 6–7 Å in proteins and 2–3 Å in water. R_c for water corresponds approximately to the size of a water molecule. The R_c value for proteins is larger, as expected.

Structural heterogeneity versus dynamical disorder.— Does the increase in dynamical electronic-coupling disorder with donor-acceptor distance reduce structural electronic-coupling disorder at large distances? That is, do differences in $\langle T_{\mathrm{DA}}^2 \rangle$ among ET species become less pronounced, on average, for $R_{\mathrm{DA}} > R_c$? Figure 3 shows the influence of structural electronic-coupling disorder as a function of R_{DA} for the water-mediated and protein-mediated ET systems. It is a plot of the structural disorder parameter $S[X] = \sqrt{\mathrm{var}[X]}/\mathrm{avg}[X]$ for $X = \langle T_{\mathrm{DA}}^2 \rangle$ [Eq. (2)], $X = \langle T_{\mathrm{DA}} \rangle^2$, $X = \sigma^2$, and $X = k_{\mathrm{ET}}$ (experimental). Figure 3 shows that $S[\langle T_{\mathrm{DA}}^2 \rangle]$ is of order 1 at all distances. This means that structural disorder is large, and its magnitude is not reduced by dynamical disorder at large distances. The experimental ET rates of the protein systems in Fig. 3 are known, and we find that $S[\langle T_{\mathrm{DA}}^2 \rangle]$ is strongly correlated with $S[k_{\mathrm{ET}}]$. Therefore, the variability of the ET rates at a given distance reflects structural disorder in the electronic coupling. Interestingly, the structural disorder parameters of $\langle T_{\mathrm{DA}}^2 \rangle$, $\langle T_{\mathrm{DA}} \rangle^2$, and σ^2 are of similar magnitudes and are highly correlated with one another for both protein- and water-bridged tunneling. Thus, the heterogeneity in $\langle T_{\mathrm{DA}}^2 \rangle$ values at each distance arises equally from $\langle T_{\mathrm{DA}} \rangle^2$ and σ^2. The bridge-mediated donor-acceptor electronic coupling fluctuations show the same sensitivity to the underlying molecular geometry as does the average coupling, implying a connection between structural motifs and the coupling fluctuations related to the motion of the motifs.

To summarize, electronic coupling is most likely determined by nonequilibrium geometries of the system beyond a critical distance (6–7 Å in proteins and 2–3 Å in water). In this dynamical disorder regime, the average structure cannot be used to compute the electronic-coupling strength. However, even when nonequilibrium conformations determine the coupling, the coupling fluctuations depend strongly on the underlying equilibrium structure. Therefore, dynamical electronic-coupling disorder does not wash out structural electronic-coupling disorder (the structural heterogeneity of $\langle T_{\mathrm{DA}}^2 \rangle$) in tunneling-mediated protein ET. In addition to tunneling, resonant and multistep hopping transport mechanisms can arise in protein [25] and DNA [26] ET under some circumstances. In these other regimes, the donor-acceptor interactions are expected to be particularly sensitive to dynamical disorder.

The research is supported by NIH grant GM-048043 and, in part, by the Duke Center for Theoretical and Mathematical Sciences and by the University of Cyprus. We thank Dr T. R. Prytkova and Dr. J. Lin for providing some of the simulation data and Professor G. Archontis for helpful discussions.

*ilya.balabin@duke.edu
+david.beratan@duke.edu
‡skourtis@ucy.ac.cy

[1] *Biological Inorganic Chemistry: Structure and Reactivity*, edited by I. Bertini, H. B. Gray, E. I. Stiefel, and J. S. Valentine (University Science, Sausalito, CA, 2007).
[2] *Electron Transfer from Isolated Molecules to Biomolecules*, Advances in Chemical Physics Vol. 106 (John Wiley & Sons, New York, 1999), Parts 1 and 2.
[3] A. Warshel and W. W. Parson, Q. Rev. Biophys. **34**, 563 (2001).
[4] V. S. Pande and J. N. Onuchic, Phys. Rev. Lett. **78**, 146 (1997).
[5] M. Bixon and J. Jortner, Russ. J. Electrochem. **39**, 3 (2003).
[6] J.-M. Lopez-Castillo, A. Filali-Mouhim, I. L. Plante, and J.-P. Gerin, J. Phys. Chem. **99**, 6864 (1995).
[7] M. Kemp, A. Roitberg, V. Mujica, T. Wanta, and M. A. Ratner, J. Phys. Chem. **100**, 8349 (1996).
[8] S. S. Skourtis, J. Lin, and D. N. Beratan, in *Modern Methods for Theoretical Physical Chemistry of Biopolymers*, edited by E. B. Starikov, S. Tanaka, and J. P. Lewis (Elsevier, New York, 2006), pp. 357–379.
[9] H. B. Gray and J. R. Winkler, Q. Rev. Biophys. **36**, 341 (2003).
[10] J. Lin, I. A. Balabin, and D. N. Beratan, Science **310**, 1311 (2005).
[11] R. A. Marcus and N. Sutin, Biochim. Biophys. Acta **811**, 265 (1985).
[12] I. A. Balabin and J. N. Onuchic, Science **290**, 114 (2000).
[13] A. Troisi, M. A. Ratner, and A. Nitzan, J. Chem. Phys. **119**, 5782 (2003).
[14] S. S. Skourtis, I. A. Balabin, T. Kawatsu, and D. N. Beratan, Proc. Natl. Acad. Sci. U.S.A. **102**, 3552 (2005).
[15] T. R. Prytkova, I. V. Kurnikov, and D. N. Beratan, Science **315**, 622 (2007).
[16] See EPAPS Document No. E-PRLTAO-101-059841 for supporting material. For more information on EPAPS, see http://www.aip.org/pubservs/epaps.html.
[17] K. Yates, *Hückel Molecular Orbital Theory* (Academic, New York, 1978).
[18] A. Vela and J. L. Gazquez, J. Phys. Chem. **92**, 5688 (1988).
[19] S. S. Skourtis and D. N. Beratan, in Ref. [2], Part 1, pp. 377–452.
[20] A. A. Stuchebrukhov, Theor. Chem. Acc. **110**, 291 (2003).
[21] I. A. Balabin and J. N. Onuchic, J. Phys. Chem. **100**, 11 573 (1996).
[22] A. Teklos and S. S. Skourtis, J. Chem. Phys. **125**, 244103 (2006).
[23] T. Hesterberg, D. S. Moore, S. Monaghan, A. Clipson, and R. Epstein, *Bootstrap Methods and Permutation Tests* (W. H. Freeman and Company, New York, 2005), 2nd ed.
[24] J. K. Taylor and C. Cihon, *Statistical Techniques for Data Analysis* (CRC Press, Boca Raton, FL, 2005), 2nd ed.
[25] C. Shih *et al.*, Science **320**, 1760 (2008).
[26] E. Hatcher, A. Balaeff, S. Keinan, R. Ventkatramani, and D. N. Beratan, J. Am. Chem. Soc. **130**, 11 752 (2008).